Tissue Oxygenation Changes to Assess Healing in Venous Leg Ulcers Using Near-Infrared Optical Imaging

Rebecca Kwasinski,[1] Cristianne Fernandez,[1] Kevin Leiva,[1] Richard Schutzman,[1] Edwin Robledo,[1] Penelope Kallis,[2] Luis J. Borda,[2] Robert Kirsner,[2] Francisco Perez-Clavijo,[3] and Anuradha Godavarty[1,*]

[1]*Optical Imaging Laboratory, Department of Biomedical Engineering, Florida International University, Miami, Florida.*
[2]*Department of Dermatology, UM Wound Care Center, University of Miami, Miami, Florida.*
[3]*Podiatry Care Partners, Inc., Doral, Florida.*

Anuradha Godavarty, PhD

Submitted for publication October 8, 2018. Accepted in revised form March 13, 2019.

*Correspondence: Optical Imaging Laboratory, Department of Biomedical Engineering, Florida International University, 10555 W Flagler St, Miami, FL 33174
(e-mail: godavart@fiu.edu).

Objective: Venous leg ulcers (VLUs) comprise 80% of leg ulcers. One of the key parameters that can promote healing of VLUs is tissue oxygenation. To date, clinicians have employed visual inspection of the wound site to determine the healing progression of a wound. Clinicians measure the wound size and check for epithelialization. Imaging for tissue oxygenation changes surrounding the wounds can objectively complement the subjective visual inspection approach. Herein, a handheld noncontact near-infrared optical scanner (NIROS) was developed to measure tissue oxygenation of VLUs during weeks of treatment.
Approach: Continuous-wave-based diffuse reflectance measurements were processed using Modified Beer-Lambert's law to obtain changes in tissue oxygenation (in terms of oxy-, deoxy-, total hemoglobin, and oxygen saturation). The tissue oxygenation contrast obtained between the wound and surrounding tissue was longitudinally mapped across weeks of treatment of four VLUs (healing and nonhealing cases).
Results: It was observed that wound to background tissue oxygenation contrasts in healing wounds diminished and/or stabilized, whereas in the nonhealing wounds it did not. In addition, in a very slow-healing wound, wound to background tissue oxygenation contrasts fluctuated and did not converge.
Innovation: Near-infrared imaging of wounds to assess healing or nonhealing of VLUs from tissue oxygenation changes using a noncontact, handheld, and low-cost imager has been demonstrated for the first time.
Conclusion: The tissue oxygenation changes in wound with respect to the surrounding tissue can provide an objective subclinical physiological assessment of VLUs during their treatment, along with the gold-standard visual clinical assessment.

Keywords: venous leg ulcers, wound healing, near-infrared imaging, optical scanner, handheld, tissue oxygenation

INTRODUCTION

Venous leg ulcers (VLUs) comprise 80% of leg ulcers[1] and affect 2.2 million Americans annually.[2] VLU incidence is increasing with age at an annual rate of 2.2% among Medicare-aged and 0.5% of younger privately insured Americans.[3] Typical risk factors tend to include older age, obesity, previous leg injuries,

DOI: 10.1089/wound.2018.0880

deep venous thrombosis, and phlebitis.[4] VLUs can last from weeks to years and tend to recur.[5] They are mainly diagnosed clinically through comprehensive history and physical examination, with confirmatory venous studies (reflux studies).

Chronic venous insufficiency caused by sustained ambulatory venous pressures (aka venous hypertension) is common in the obesity, those with sedentary lifestyle, and leads to a diseased venous system and eventually to venous ulceration.[6] Clinical evaluation and initial management of VLUs are summarized in Fig. 1. Noninvasive diagnostic tests such as duplex ultrasound (DUS) are used as a gold standard to evaluate reflux in venous ulcers. These tests can evaluate venous anatomy, and aid or confirm the presence of venous insufficiency and reflux,[7] such that the gold-standard compression therapy can begin upon the onset of venous ulceration.

Compression therapies are typically performed during weeks 0–4 of VLU treatment. Currently, physicians assess healing status of chronic wounds by simple visual inspection (wound coloration, texture, and epithelialization) and wound size measurements.[8,9] Effectiveness of compression therapy in the healing of the wound is likewise monitored through visual assessment and wound size measurements at times of weekly wound dressings. Typically if a wound is not 30% smaller by week 4, it is unlikely to heal by week 12, and such patients are then reassessed or referred for further diagnosis and appropriate management (through advanced therapies along with continued compression).[10] About 50–67% of VLU patients exhibiting decreased wound size during the first month of compression therapy will be healed after 6 months treatment,[11] but many VLUs remain refractory to compression treatment as measured by wound size/area.

Studies have been performed in the past using different imaging devices with the aim to complement the visual inspection done by clinicians with physiological assessments of VLUs and their surroundings. The different imaging modalities used in recent studies have included confocal laser scanning microscopy (or confocal microscopy), optical coherence tomography, hyperspectral imaging (HSI), orthogonal polarization spectral imaging, thermal imaging, multispectral imaging (MSI), remittance spectroscopy, laser Doppler, and near-infrared (NIR) imaging[12–25] (Table 1). Different modalities assess different parameters in VLUs, such as bacterial infection, fibrin deposits, tissue oxygenation or oxygen saturation (StO_2), capillary morphology, perfusion, or skin temperatures to differentiate

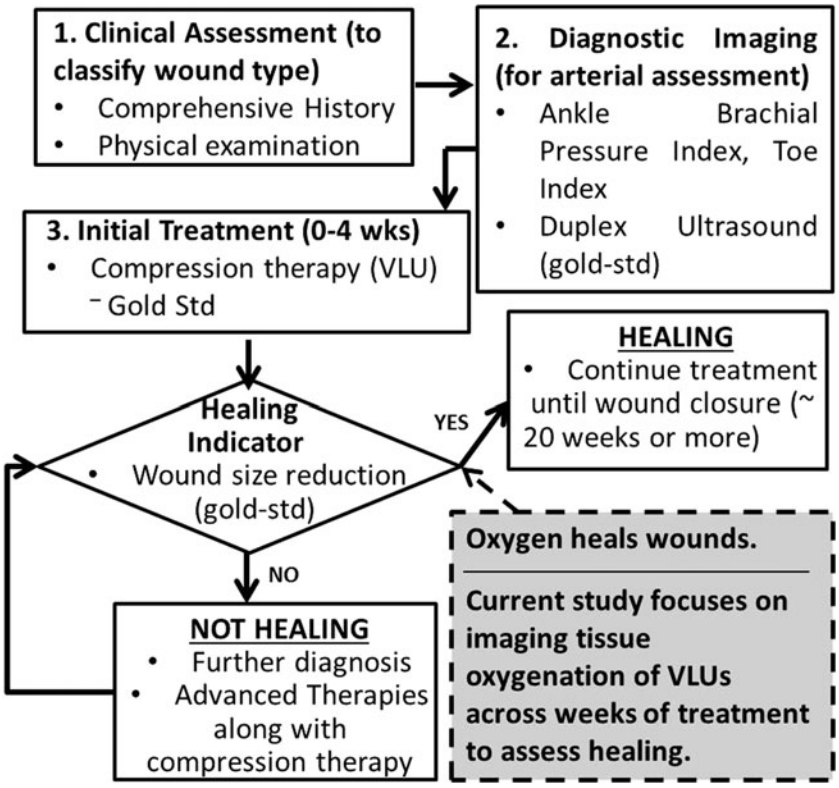

Figure 1. Flow chart showing standard clinical evaluation of VLUs and its initial management. VLUs, venous leg ulcers.

Table 1. *Summary of optical-based imaging modalities employed to assess venous leg ulcers*

Imaging Modality	*Measured Parameter(s)*	*Major Finding(s)*
CLSM	Distance of bacterial aggregates to VLU surface	Distribution of the bacteria in the chronic wounds was nonrandom.[12]
Confocal microscopy	Distribution of fibrin deposits	Distribution of fibrin deposition was highly variable and patchy. Marginal or patchy fibrin deposition might have a greater effect on the exchange of oxygen and other nutrients between blood and dermis.[13]
Optical coherence tomography	*In vivo* blood vessels of superficial skin layers; pattern of perfusion	In chronic venous insufficiency, different stages of vascularization are visible. For instance, in the middle of the wound itself, granulation islands with larger aggregations of vessels in the form of dots, blobs, and coils are apparent.[14]
Hyperspectral imaging	Tissue oxygenation as oxy- and deoxyhemoglobin, and/or oxygen saturation maps (415–990 nm)	Possible to identify necrotic regions using oxygenation, and increased oxygenation at wound bed.[15] Two statistical approaches (spectral angle mapping and k-means clustering) were used to compare wound segmentation with dermatologist assessment. K-means was more stable and reliable method to classify wound regions.[16]
Orthogonal polarization spectral imaging	Capillary morphology, density, and diameter	Capillary morphology and capillary diameter were substantially different between the venous ulcer patients and normal subjects.[17]
Multispectral imaging	Skin oxygenation as oxygen saturation	Reduction of oxygen saturation after wound healing from weeks 1 to 14.[18]
Laser Doppler imaging	LDF (or perfusion)	Elevated basal LDF and preserved maximal LDF during reactive hyperemia were found in perimallerolar skin of patients with healing VLU.[19] Changes in LDF during leg elevation and arterial occlusion were significantly reduced in patients with VLUs.[20] Granulated tissue inside VLU had high laser Doppler area flux than nongranulated tissue and adjacent/distance skin from VLU.[21] LDA (similar to LDF) showed no significant differences between VLU patients and control group.[22]
Remittance spectroscopy	Hemoglobin and water absorption	A high absorption and low remittance pointed to a large amount of granulation tissue and oxyhemoglobin doublet peak represents open wound area.[23]
Thermal imaging	Skin temperatures	Higher temperature is observed at the onset of VLU.[24]
Near-infrared optical imaging	Diffuse reflectance optical contrast	Healing and nonhealing VLUs showed a distinct difference in diffuse reflectance optical contrasts.[25]

CLSM, confocal laser scanning microscopy; LDA, laser Doppler anemometer; LDF, laser Doppler flux; VLU, venous leg ulcer.

healing and nonhealing regions, or determine factors that impact healing.

Of the many important parameters that play a key role in wound assessment during treatment, increased tissue oxygenation is one of the key parameters that can promote healing. HSI, MSI, and NIR optical imaging are the three imaging modalities that can measure tissue oxygenation changes in the wounds. While HSI involved visible and infrared wavelengths (400–1,100 nm) MSI employed visible and NIR wavelengths (460–886 nm) during imaging of VLUs. Cutaneous oxygenation maps of identified necrotic regions, as well as reducing oxygen saturation, were observed with weeks of healing.[18] Although HSI and MSI employ NIR wavelengths in their spectrum, the oxygenation measurements across all wavelengths are combined to provide skin oxygenation (as visible light is absorbed predominantly in the cutaneous skin layer). On the contrary, NIR optical imaging uses only the NIR spectrum of HSI and MSI, with specific wavelengths chosen to obtain subcutaneous oxygenation maps of wounds.

NIR light (between 650 and 900 nm) is nonionizing and minimally absorbed by tissues, allowing its deeper penetration, and preferentially scattered by major tissue components (oxygenated hemoglobin [HbO], deoxygenated hemoglobin [HbR], and water), which will enable mapping of physiological changes in wound healing through measurement of HbO and HbR. In this study, NIR optical imaging was performed to image for physiological changes in terms of tissue oxygenation across weeks of VLU treatment. To date, large MSI and HSI devices have been used for wound imaging, using a broad spectrum of wavelengths. In this work, we are able to observe changes in oxygenation from few specific (narrow band) wavelengths and in the NIR regions (to allow subsurface imaging, unlike MSI or HSI that predominantly employs visible light wavelengths). Use of only specific narrow band of wavelengths in the NIR region allows the device to be developed as a low-cost, handheld imaging tool that can be readily accessible to assess wound healing in dressing rooms, making it a more practical instrument for clinical applications.

In our past work at Optical Imaging Laboratory, noncontact NIR optical imaging studies were performed using a low-cost, handheld, near-infrared optical scanner (NIROS).[25] Initial studies were performed using a single-wavelength NIR light source, and diffuse reflectance optical contrasts were determined between wound and periwound to differentiate healing versus nonhealing VLUs.

Imaging studies were performed by varying distances and angles of the device with respect to the wound causing a change in the illumination source intensity on the wounds. In spite of the varied imaging conditions, a distinct difference in optical contrasts between healing (positive contrasts) versus nonhealing (negative contrasts) VLUs was consistently observed.[25] Herein, tissue oxygenation measurements (as oxy-, deoxy-, total hemoglobin [HbT], and oxygen saturation) are obtained using a modified dual-wavelength NIROS to determine if these oxygenation parameters in VLUs and their surroundings can assess healing from longitudinal imaging studies.

CLINICAL PROBLEM ADDRESSED

VLUs are primarily diagnosed clinically through comprehensive history and physical examination, with confirmatory venous studies (reflux studies). However, oxygen is vital for the healing of wounds. There is a need for a physiological approach to assess oxygenation to the wounds during treatment. Herein, an NIR optical imaging approach was developed to obtain changes in oxy-, deoxy-, total hemoglobin, and oxygen saturation measurements in and around the VLUs. These subclinical physiological assessments can potentially complement the gold-standard clinical assessment, since physiological changes in tissue oxygenation manifest before visual changes in VLU's size and extent of epithelialization.

MATERIALS AND METHODS

Instrumentation

A continuous-wave (CW), noncontact, handheld-based NIROS was developed for tissue oxygenation imaging of VLUs in the clinic. The handheld NIROS utilizes a multiwavelength light-emitting diode (LED) light source ([660–735–805–940] ± 20–45 nm bandwidth), which is operated at dual wavelength (725, 797 nm) for this study (Fig. 2). The optical power of the LED on the illumination surface is <5 mW. An Arduino-based LED driver controls the LED light source to multiplex between the two wavelengths at a frequency of 10 Hz, and illuminates the wound and its surroundings. The LED driver was also used to optimize the source to maximize the optical power, leading to 725 and 797 nm as the two specific wavelengths (chosen for the dual wavelength imaging between 700 and 830 nm). The area of illumination encompassing both these wavelengths was determined from the region of overlap across the two illuminated wavelengths. Since a single LED was used, this area of illumination was limited to <4 cm^2, limiting the ability to image the entire region of large wounds.

Diffuse reflectance signals from the tissue surface are detected using an NIR-sensitive complementary metal-oxide semiconductor (CMOS) camera (IDS), after these signals pass a long pass filter (LP645; MidOpt) and a focusing lens. A custom-developed Matlab graphical user interface (GUI) synchronizes the source and detector to acquire images at a frame rate of 10 Hz. NIROS was stabilized using an articulating arm during imaging studies. A separate endoscopic camera was used to acquire digital white light images of the VLU and its surroundings. The developed GUI acquired the detected signals from both wavelengths, and employed modified Beer-Lambert's law (MBLL) to determine changes in oxy- (ΔHbO) and deoxyhemoglobin (ΔHbR) across the entire wound.

Subject recruitment

Longitudinal imaging studies across weeks of treatment were carried out on three patients with one or more VLUs (between 55 and 88 years of age).

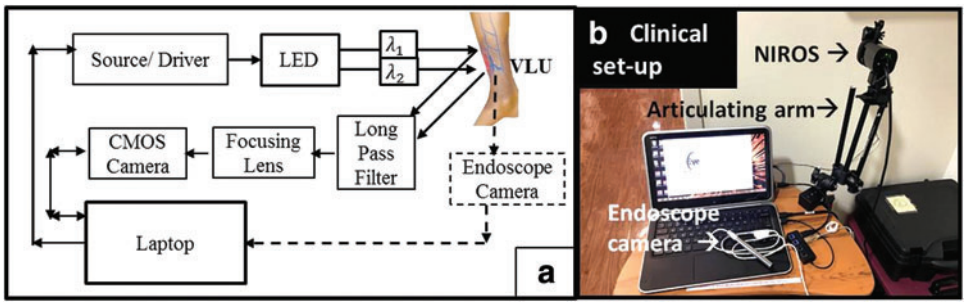

Figure 2. **(a)** Schematic of the portable, handheld NIROS for noncontact area imaging of VLUs. A separate endoscope camera used sequentially to obtain white light images of the wounds. **(b)** Clinical setup of NIROS during VLU imaging studies. NIROS, near-infrared optical scanner. Color images are available online.

Subjects were recruited at Podiatry Care Partners, Inc. and the University of Miami Wound Care Center through FIU and UM Institutional Review Board (IRB) approvals. A written consent was obtained from all participating subjects, and their medical records accessed through Health Insurance Portability and Accountability Act (HIPAA) authorization. Clinical evaluation status of the recruited VLU cases is provided in Table 2.

Healing was assessed based on visual inspection of the wound, wound size reduction during the treatment process (even if it were slow), and appearance of granulation (or epithelialization) and skin coloration during healing. Week 1 in Table 2 depicts the first week that the subject was recruited and imaged. The onset of VLU was calculated backward from the recruited week. All the subjects had no arterial deficiency, as assessed from their pedal pulses (pulse obtained near the ankle), skin temperature, and capillary refill time by the clinician. VLU cases 2 and 3 (from the same patient) were nonhealing when the imaging studies began, and soon were assessed as healing during weeks of treatment. VLU cases 1 and 4 were already assessed as healing when the subjects were recruited. In case 4, the VLU was diagnosed as healed by week 18 after the imaging study began; hence, the wound measurements were not acquired therefrom. However, the subject was still seen at the clinic since there was an epithelial arrest of the wound. The VLU epithelialized but the epidermis was not maturing.

Data acquisition

Each of the 4 VLUs was imaged during the respective weeks as provided in Table 2. Although the subjects were clinically treated at the wound center each week, they were not compliant or available to participate in the imaging study each week. Imaging was performed at least three times during each visit with variations in angle/location of the device with respect to the wound, to pick the best data set with minimal glare effects (or specular reflection). Subjects were imaged on a standard reclining chair, with the device's location adjusted to accommodate the field of view of the VLU with-

Table 2. *Wound size and healing status of venous leg ulcer cases imaged using a near-infrared optical scanner across weeks of treatment*

			Wound Measurements			
VLU Case No.	*Wound Onset*	*Week Imaged*	L×W *(cm)*	*Area (cm^2)*	*Depth (cm)*	*H/NH*
1	One-month history (78M)	1	4.4×4.0	17.6	0.2	H
		3	3.5×3.4	11.9	0.1	H
		5	2.0×2.5	5	0.1	H
		14	0.5×0.4	0.2	0.1	H
2	Ten-month history (55M)	1	4.7×2.1	9.87	0.3	NH
		3	4.0×1.6	6.4	0.3	NH
		12	2.6×2.7	7.02	0.2	H
		13	2.1×0.8	1.68	0.2	H
		24	1.4×1.1	1.54	0.3	H
		38	1.3×1.0	1.3	0.3	H
		39	1.3×1.0	1.3	0.3	H
3	Ten-month history (55M)	1	1.3×0.4	0.52	0.2	NH
		9	1.5×0.9	1.35	0.2	NH
		10	1.2×0.3	0.36	0.2	H
		21	0.7×0.2	0.14	0.2	H
		35	0.6×0.1	0.06	0.2	H
		36	0.5×0.1	0.05	0.1	H
4	Eight-month history (88F)	1	3.1×1.4	4.34	0.1	H
		3		—		Healed week 18 onward; epithelial arrest (epithelialized but epidermis not maturing)
		18		—		
		20		—		
		22		—		
		27		—		
		29		—		
		30		—		
		31		—		
		36		—		
		37		—		
		38		—		

H, healing; NH, nonhealing.

out any additional movement by the subject. The wound was cleaned and debrided by the treating physician before imaging. Reference markers of known size were placed around the VLUs during imaging, to orient the wound obtained from NIR imaging to the white light (or digital color) image of the ulcers (and ongoing coregistration studies, unpublished).

During each imaging study, the dual-wavelength LED illuminated the tissue region encompassing the VLU and its surroundings (*i.e.*, wound and background), and diffuse-reflected signal was acquired at each wavelength [$I(x,y,\lambda_i)$]. These diffuse reflectance images were calibrated using a uniformly diffusing calibrating sheet before imaging each VLU, to account for the source illumination distribution during imaging. Digital white light images of the VLU and its surroundings were acquired using the endoscope camera during each imaging visit. In some cases, the VLUs were larger than the area of illumination by the LED source. Hence, the field of view of NIROS was adjusted, such that it can view as much of the VLU and the immediate surrounding normal tissue, to obtain the contrast in tissue oxygenation during longitudinal comparison study (Image analysis section).

Image analysis

MBLL was used to calculate the changes in oxy- (ΔHbO) and deoxyhemoglobin (ΔHbR) from the diffuse reflectance images of the tissue. This law is an empirical description of optical attenuation in a highly scattering medium.[26,27] The change in optical density (*OD*; or apparent absorption) of the tissue $\Delta OD(x,y,\lambda_i)$ at the spatial coordinate (x,y) and at each wavelength λ_i is thus calculated using diffuse reflectance intensity from the tissue and accounting for the dark noise [$I_D(x,y)$] and the calibration factor [$I_{cal}(x,y,\ \lambda_i)$], which is given by Equation (1).

$$OD(x,y,\lambda i) = -\log \frac{I_{\lambda i}(x,y) - I_D(x,y)}{I_{cal\lambda i}(x,y) - I_D(x,y)}. \quad (1)$$

By measuring ΔOD at two wavelengths (λ_1 and λ_2) and using extinction coefficients of oxyhemoglobin, $\varepsilon_{HbO}(\lambda_i)$, and deoxyhemoglobin, $\varepsilon_{HbR}(\lambda_i)$, at the respective wavelengths, concentration changes of oxy- (ΔHbO) and deoxyhemoglobin (ΔHbR) can be determined.[26,27]

$$\Delta HbO\ (x,y) = \frac{\left\{\varepsilon_{HbR}^{\lambda_1}\ \Delta OD^{\lambda_2} - \varepsilon_{HbR}^{\lambda_2}\ \Delta OD^{\lambda_1}\right\}}{\left\{\left(\varepsilon_{HbR}^{\lambda_1}\varepsilon_{HbO}^{\lambda_2} - \varepsilon_{HbR}^{\lambda_2}\varepsilon_{HbO}^{\lambda_1}\right)LB\right\}} \quad (2)$$

$$\Delta HbR\ (x,y) = \frac{\left\{\varepsilon_{HbO}^{\lambda_2}\ \Delta OD^{\lambda_1} - \varepsilon_{HbO}^{\lambda_1}\ \Delta OD^{\lambda_2}\right\}}{\left\{\left(\varepsilon_{HbR}^{\lambda_1}\varepsilon_{HbO}^{\lambda_2} - \varepsilon_{HbR}^{\lambda_2}\varepsilon_{HbO}^{\lambda_1}\right)LB\right\}}, \quad (3)$$

where L is the mean free path, and B is the pathlength factor. In the current studies, the differences in oxy- and deoxyhemoglobin concentrations of the wound to periwound site are compared each week. Hence, effective values of changes in oxy- and deoxyhemoglobin [estimated as $\Delta HbO(x,y)_{eff} = \Delta HbO(x,y)LB$ and $\Delta HbR(x,y)_{eff} = \Delta HbR(x,y)LB$] are used for further analysis, where the unknown factors L and B are grouped. The effective changes in total hemoglobin and oxygen saturation are estimated from the normalized $\Delta HbO(x,y)_{eff}$ and $\Delta HbR(x,y)_{eff}$ as follows:

$$\Delta HbT(x,y)_{eff} = \Delta HbO(x,y)_{eff} + \Delta HbR(x,y)_{eff} \quad (4)$$

$$StO_2(x,y)_{eff} = \Delta HbO(x,y)_{eff} / \Delta HbT(x,y)_{eff}. \quad (5)$$

The estimated tissue oxygenation parameters were in turn plotted as two-dimensional (2D) spatial maps (normalized and scaled appropriately) for each VLU and visit, across weeks of treatment. All these parameters described here on are only the effective changes. For simplicity, all effective tissue oxygenation parameters will be labeled without the suffix (*eff*) for the rest of the article.

Differences in tissue oxygenation between wound and immediate normal tissue around it (*i.e.*, background) are evaluated in terms of optical contrasts. These optical contrasts between wound and background (*W*:*B*) were determined by selecting a 10×10 pixel area within the wound and the immediate surrounding regions (randomly at three locations around the wound and within the region encompassed by the markers).[25] The extent of change in tissue oxygenation of the VLU in comparison with the immediately surrounding normal tissue was obtained by estimating the optical contrast in terms of effective hemoglobin concentrations. A Weber-based wound to background (*W*:*B*) optical contrast was used on the average intensity of each tissue oxygenation (*TO*) parameter at the selected region of interest (ROI of 10×10 pixels) within the visible wound and surrounding tissue as given below:

$$[W:B]_{TO} = \frac{W_{TO} - B_{TO}}{B_{TO}} x\ 100\%. \quad (6)$$

The *W*:*B* optical contrast was calculated thrice for each imaged VLU (per visit), by using three randomly chosen ROIs of background tissue in comparison with the ROI of the wound. Three different backgrounds were chosen to determine variability in the contrast data, which may arise from the operator's choice of background ROI (that can vary in intensity from nonuniform source illumination and/or specular reflection).

RESULTS

2D tissue oxygenation maps (in terms of ΔHbO, ΔHbR, ΔHbT, and StO_2 maps) along with white light images are shown for one healing (case 1) and one nonhealing VLU (case 2) on the first week and last week of their recruitment in Figs. 3 and 4, respectively. Three markers are placed around the wound to help locate the wound in the NIR images. The jet colored regions in the maps is where oxy-

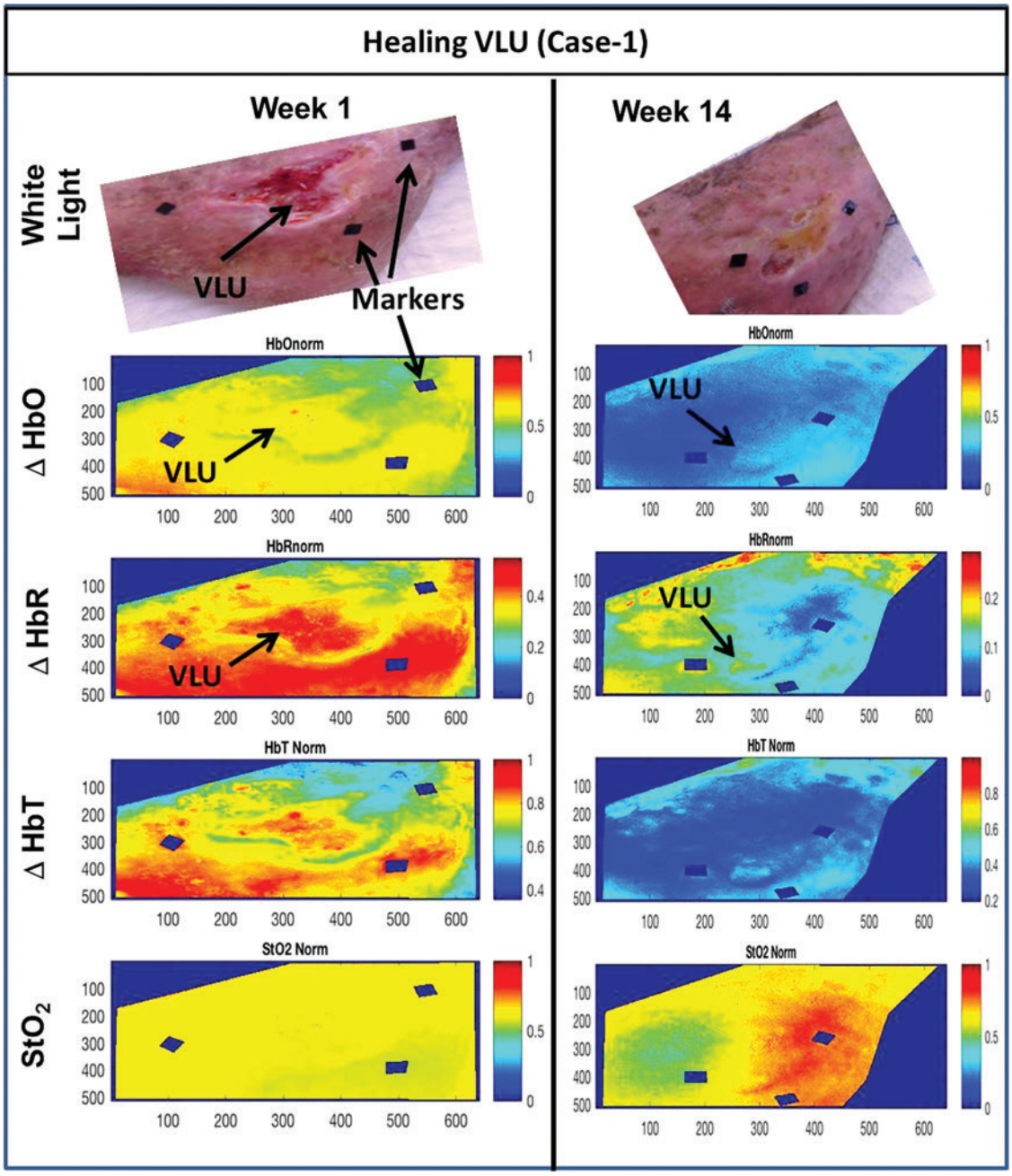

Figure 3. White light images (*top row*), normalized ΔHbO maps (*second row*), normalized ΔHbR maps (*third row*), normalized ΔHbT maps (*fourth row*), and normalized StO_2 maps (*fifth row*) for healing VLU (case 1) at the first and last week of imaging. HbO, oxygenated hemoglobin; HbR, deoxygenated hemoglobin; HbT, total hemoglobin; StO_2, oxygen saturation. Color images are available online.

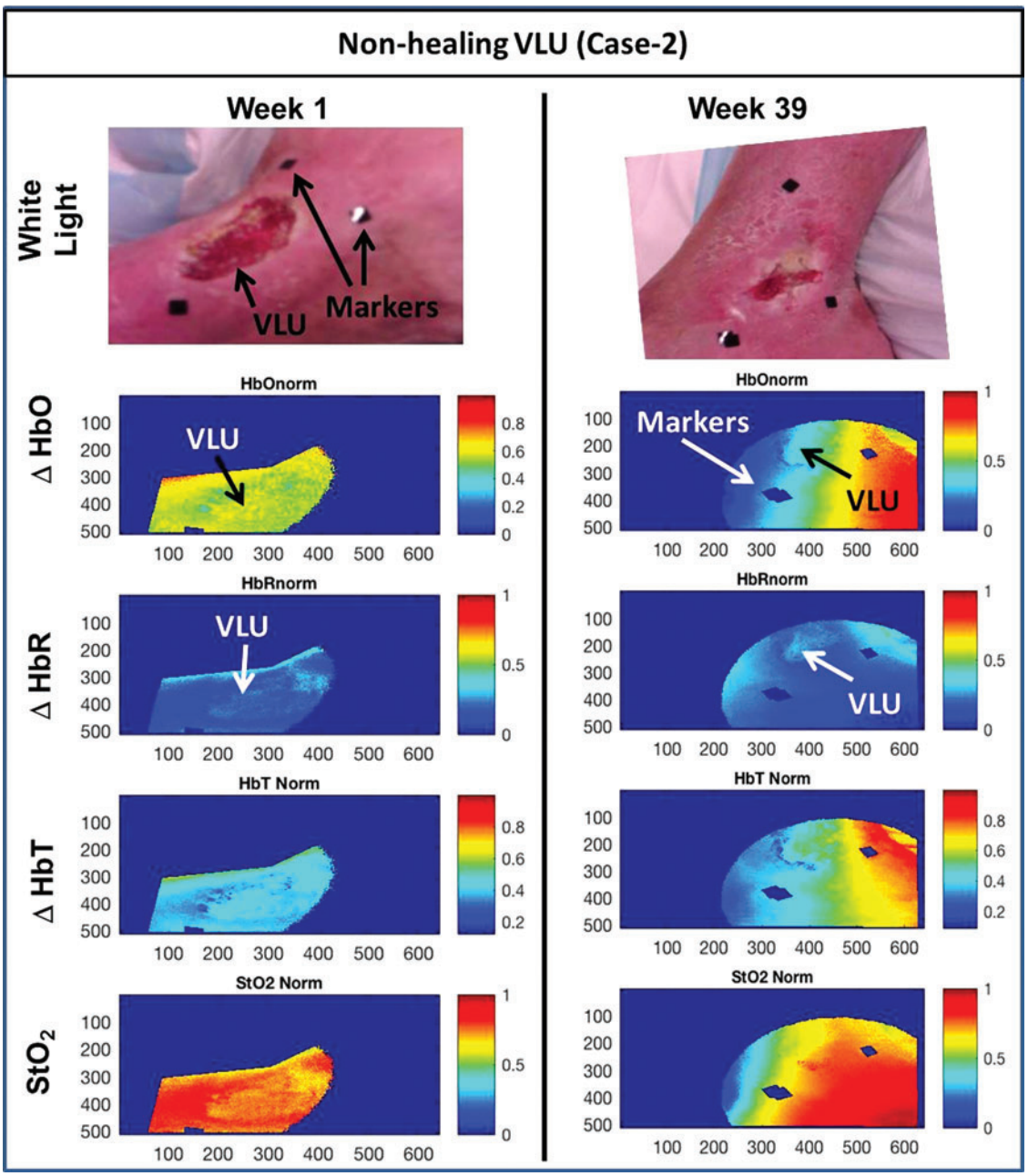

Figure 4. White light images (*top row*), normalized ΔHbO maps (*second row*), normalized ΔHbR maps (*third row*), normalized ΔHbT maps (*fourth row*), and normalized StO_2 maps (*fifth row*) for nonhealing VLU (case 2) at the first and last week of imaging. Color images are available online.

genation parameters were determined, and these were overlaid onto the detector's field of view.

In the case of the healing VLU (case 1), the normalized maps of $\Delta HbO(x,y)$ depicted an increased concentration to the wound site compared with most of the immediate surroundings of the wound (*i.e.*, termed "background"). This difference in ΔHbO concentration almost disappears as the wound heals by the last week. Similar contrasts between the wound and background were observed in other tissue oxygenation parameters during first week, but this contrast was negligible by the last week of recruitment into the study.

In the case of the nonhealing VLU (case 2), it was a large VLU, and hence the entire wound was not under the field of view of imaging. Since the focus of our study was on assessing differences in oxygenation between wound and background across weeks, the field of view was adjusted to include a portion of the wound and its immediate surround-

ings. In Fig. 4, the normalized maps of $\Delta HbO(\underline{x},y)$ depict an increased concentration to the wound site compared with the background. Even by the end of the last week of recruitment, there was a difference in ΔHbO concentration between wound and background region. Similar differences in wound to background contrasts remained (either increased or decreased) for other tissue oxygenation parameters even after weeks of treatment and the last week of our recruitment study. This VLU (case 2) was still open and not healed even after a year from the last week of our recruitment for the imaging study. The qualitative, 2D tissue oxygenation pseudocolor maps did not display an obvious visual contrast in some cases (*e.g.*, Fig. 4). Hence, qualitative maps were quantified as optical contrast maps, and the changes in tissue-oxygenation-based *W*:*B* contrasts were estimated across weeks of imaging and treatment.

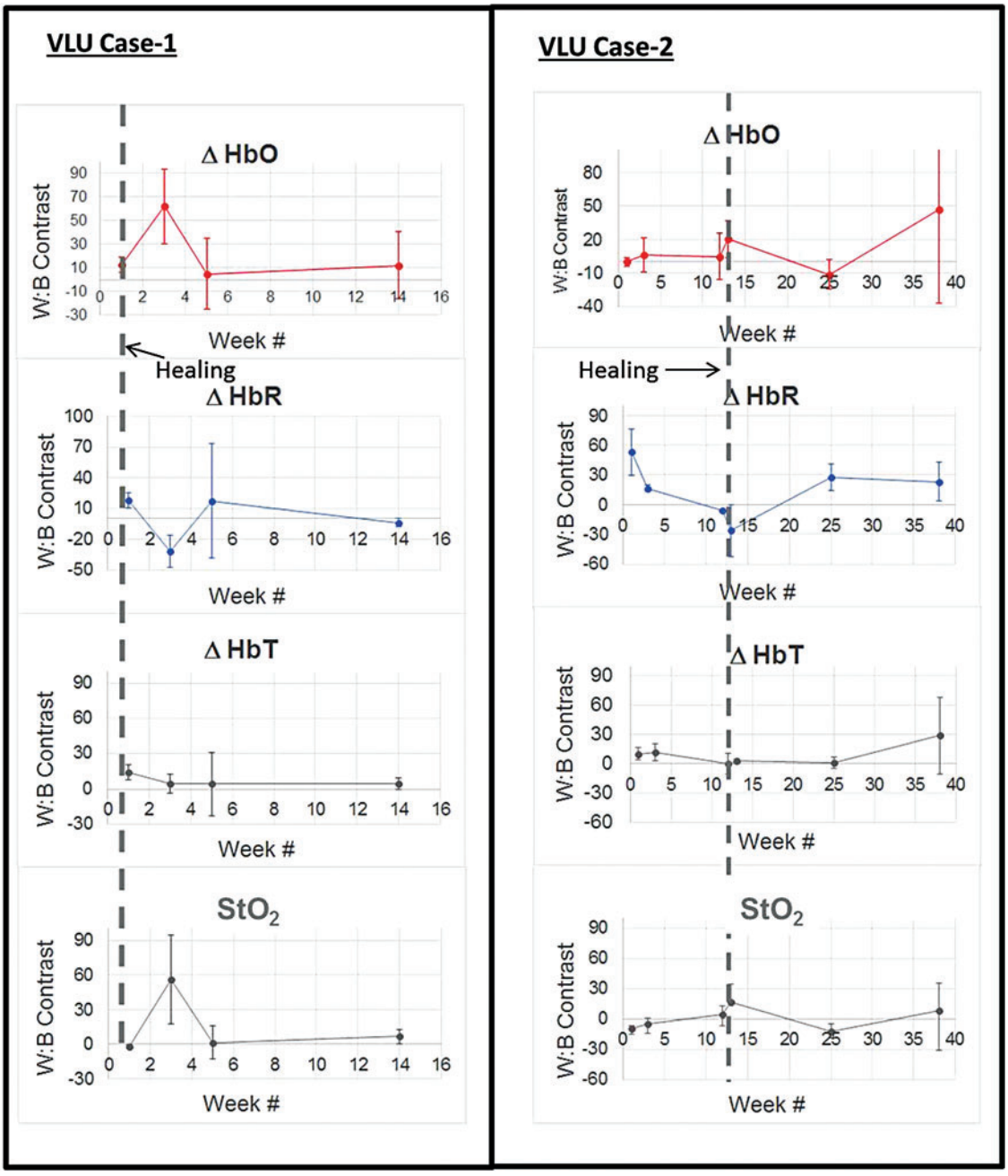

Figure 5. Average wound to background (*W*:*B*) contrast in terms of various tissue oxygenation parameters across weeks of treatment for VLU cases 1 and 2. The *gray dashed line* at a given week No. is when the VLU was diagnosed as healing by the clinician. Color images are available online.

Quantitative assessment of *W*:*B* contrasts across each recruited week of the treatment for all the four VLU cases is shown in Fig. 5 (for cases 1 and 2) and Fig. 6 (for cases 3 and 4) for each of the normalized tissue oxygenation parameters. The average and the standard deviation across the three estimations of *W*:*B* (based on three randomly located backgrounds as described in Materials and Methods section) were determined. In both Figs. 5 and 6, the gray dashed line at a given week No. is when the VLU was diagnosed as healing by the clinician. In case 4 (Fig. 6), the gray dotted line at week 18 represents a healed VLU, as clinically diagnosed.

In case 1, the *W*:*B* optical contrast stabilized and almost approached zero in each tissue oxygenation parameter, across weeks of treatment of the healing VLU. In case 2, although the clinician assessed the wound as healing (but slow), $\Delta HbO(x,y)$ *W*:*B* contrast was unstable, increased, and did not converge to zero. A similar increase in $\Delta HbT(x,y)$ *W*:*B* contrast was observed, although no major differ-

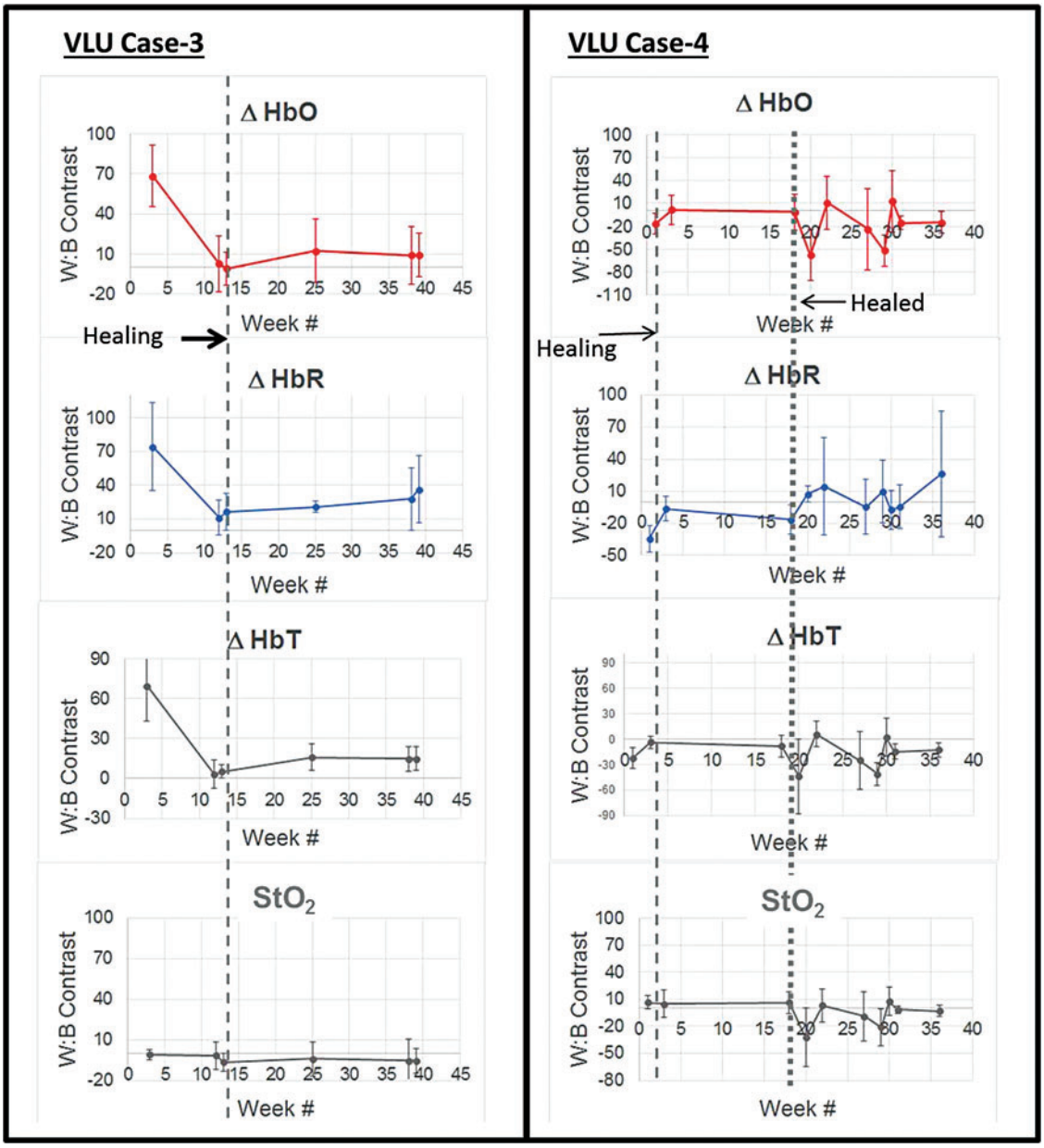

Figure 6. Average wound to background (*W*:*B*) contrast in terms of various tissue oxygenation parameters across weeks of treatment for VLU cases 3 and 4. The *gray dashed line* at a given week No. is when the VLU was diagnosed as healing by the clinician. The *dotted gray line* at week 18 in case 4 is when the VLU was diagnosed as healed by the clinician. Color images are available online.

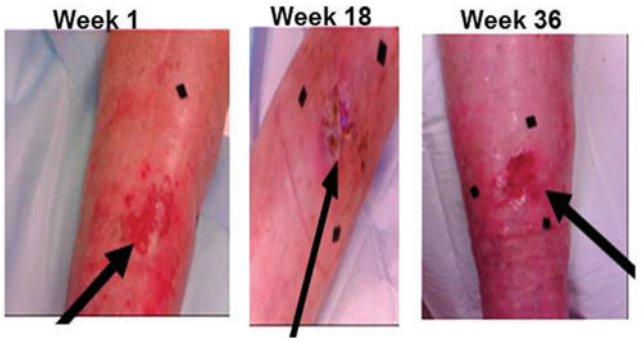

Figure 7. White light images of VLU case 4, where the wound (shown by the *black arrow*) was diagnosed as healed during week 18 of our imaging study, but the subject seen at the clinic due to an epithelial arrest, which still shows an open wound even at week 36. The *black squares* in the images are markers. Color images are available online.

ence in StO_2 was observed. The $\Delta HbR(x,y)$ increased and remained. None of the tissue oxygenation parameters converged to zero even at week 39 of our study. Although the wound was assessed as healing around week 12, the wound was not closed (see Fig. 4 for the white light image at week 39). In fact, the wound remained open even after a year from the last recruitment (*i.e.*, week 39), stating that the wound was actually nonhealing. This correlates with our tissue oxygenation contrast, which did not stabilize and converge closer to zero. This infers that the oxygenation to the wound site (in case 2) was still higher than the surrounding tissue, and that the wound has not reached normalcy from a physiological standpoint. The contrast was more distinct in oxy-, deoxy-, and total hemoglobin-based *W*:*B* contrasts, unlike oxygen saturation contrast.

In case 3, the *W*:*B* optical contrast stabilized and almost approached zero in each tissue oxygenation parameter (except a slight increase in ΔHbR, although it was much lesser than the initial contrast), across weeks of treatment of this healing VLU (similar to case 1). However, there was no distinct change in contrast in oxygen saturation-based *W*:*B* contrast in case 3. The 2D tissue oxygenation maps for this healing case 3 are included in the Appendix Fig. A1.

In case 4, the *W*:*B* contrast was close to zero in all tissue oxygenation parameters and across weeks (until week 18). Upon continuing to image this VLU for the next 18 weeks, the *W*:*B* optical contrasts were observed to fluctuate and away from a zero contrast. The wound was diagnosed as healed on week 18 of our study, and wound measurements were not acquired therefrom. However, the subject was seen in the clinic, since there was an epithelial arrest of the wound. The VLU epithelialized but the epidermis was not maturing, which was shown as increased redness in the wound region. Physiologically, this can be from increased subcutaneous ΔHbR concentrations at the VLU site compared with the background tissue (*i.e.*, increased ΔHbR *W*:*B* optical contrast), correlating with the lack of complete healing and closure of the wound. This can be seen from white light images of the VLU in case 4 shown in Fig. 7 (for weeks 1, 18, and 36). The 2D tissue oxygenation maps for case 4 are included in the Appendix Fig. A2.

DISCUSSION

From the longitudinal imaging studies on four VLU cases, it was observed that the tissue oxygenation *W*:*B* optical contrast stabilized and approached close to zero in terms of $\Delta HbO(x,y)$, $\Delta HbR(x,y)$, and $\Delta HbT(x,y)$ parameters, for healing wounds. The $StO_2(x,y)$ did not appear to be a good indicator to assess healing. For a wound that appeared healing (although at a very slow rate) but did not actually close even after a year (*i.e.*, remained nonhealing), the *W*:*B* optical contrast fluctuated and did not approach close to zero in terms of any tissue oxygenation parameters.

In the past work from a different research group, diffuse NIR spectroscopy was applied to assess the healing of another major lower extremity ulcer (diabetic foot ulcers, DFUs).[28] It was observed that as the wounds healed, the HbO and HbT concentrations at the wound locations converged to the control location measurements.[28] However, in the case of nonhealing wounds, large fluctuations in HbO and HbT concentrations at the wound location (w.r.t. control location) were observed across weeks of treatment. The current studies are in agreement with the past work in terms of observing similar trends in oxygenation contrast between wound and background (or control region) for both healing and nonhealing wounds. Although the type of lower extremity ulcer differs between the studies (VLUs vs. DFUs), the requirement of oxygen to cause healing, and that oxygen being higher at the wound site than the surrounding normal tissue during healing phase is physiologically similar across the two ulcer types.

The research studies on DFUs obtained absolute values of concentrations of HbO and HbR as point measurements at discrete point locations through contact imaging using a frequency-domain-based optical spectroscopy system.[28] On the contrary, the current imaging studies obtained effective concentrations of HbO and HbR of the wound and

surrounding areas (and not discrete point locations) through CW-based noncontact imaging. However, both the studies compare the changes in HbO at the wound to the background (or control) tissue and determine if they converge. Hence, obtaining *W*:*B* optical contrast from effective hemoglobin concentrations (as in our study) using a simpler CW instrumentation yields similar outcome as that from absolute hemoglobin concentrations (obtained from past work) using frequency-domain based optical instrumentation.

KEY FINDINGS

- Noncontact NIR imaging approach could image VLUs in real time for physiological changes in terms of tissue oxygenation, beneath the visual wound surface.
- Differences in HbO, HbR, and HbT (tissue oxygenation parameters) between wound and background across weeks of treatment was distinctly different in healing and nonhealing VLUs.
- Tissue oxygenation differences between wound and its surrounding tissues converged as the wounds healed. For nonhealing or slow-healing cases, these differences fluctuated or remained high with weeks of treatment.

This work demonstrates the potential of using a noncontact, low-cost, handheld NIR scanner for bedside real-time assessment of wound healing status through tissue oxygenation measurements. These pilot feasibility studies differentiate the trend line of tissue oxygenation changes with weeks of treatment, with the nonconvergence trend line as a major indicator of nonhealing of the wound. There is however a need to perform extensive and systematic studies on a large sample of VLU cases to demonstrate that the observed tissue oxygenation trends consistently differentiate a potential healing from a nonhealing VLU.

In addition, there is a need to develop a quantitative threshold contrast value that differentiates a potential healing wound from a nonhealing wound. The statistically significant tissue oxygenation parameter (among ΔHbO, ΔHbR, and ΔHbT) that can serve as an indicator (or biomarker) for assessing wound healing has to be determined from extensive clinical studies. Also, the effect of melanin concentrations on oxygenation measurements obtained from the unaffected skin compared to open VLUs will also be assessed. NIROS employs a single LED, limiting its area of illumination that does not encompass the entire VLU (and potentially leading to artifacts). Hence, the device is also modified with multiple LEDs to allow increased area of illumination for future studies.

INNOVATION

NIR imaging of wounds to assess healing or nonhealing of VLUs from tissue oxygenation changes using a noncontact, handheld, and low-cost imager has been demonstrated for the first time. The use of two discrete NIR wavelengths to obtain tissue oxygenation maps makes NIROS compact and handheld for practical clinical application. The portable handheld nature of NIROS has a potential for clinical use during weekly treatment of VLUs and other lower extremity ulcers during an outpatient visit, to measure tissue oxygenation changes for subclinical assessments.

CONCLUSION

A handheld noncontact-based NIROS was developed to perform CW-based diffuse reflectance imaging and measure for changes in oxy-, deoxy-, total hemoglobin, and oxygen saturation in the wound with respect to the background normal tissue. From longitudinal imaging studies across weeks of treatment of VLUs, it was observed that *W*:*B* tissue oxygenation contrast of healing wounds converged to almost zero (and stabilized). On the contrary, in a very slow-healing wound, *W*:*B* tissue oxygenation contrasts fluctuated and did not converge. Thus, the *W*:*B* optical contrast in terms of HbO, HbR, and HbT can serve as a potential biomarker to assess healing of VLUs, along with current clinical practices of measuring the reduction in wound size, and assessing for epithelialization across weeks of treatment.

Ongoing efforts are focused on performing image segmentation (and coregistration) of tissue oxygenation maps onto white light images, (*i.e.*, register onto them). This will assist in determining areas of changed oxygenation and comparing them with visual wound area. Additionally, extensive systematic VLU imaging studies are required in the future to quantify the tissue-oxygenation-based marker that can provide subclinical physiological status that objectively complements visual clinical status during its treatment.

ACKNOWLEDGMENTS AND FUNDING SOURCES

The authors acknowledge funding support from Coulter Seed Grant (BME-FIU), Coulter Under-

graduate Research Excellence (CURE) program, and Norman-Weldon Scholarship.

AUTHOR DISCLOSURE AND GHOSTWRITING

There is no conflict of interest with regard to the research in this article. The corresponding author's university (Florida International University) holds patents on the described technology. The authors listed expressly wrote the content of this article. No ghostwriters were used to write this article.

ABOUT THE AUTHORS

Rebecca Kwasinski, BS, a CURE recipient and Norman Weldon Fellow, was an undergraduate research assistant in our Optical Imaging Laboratory (OIL) at FIU, who focused on VLU and diabetic foot ulcer (DFU) imaging studies. **Cristianne Fernandez, BS,** holds similar credentials as Kwasinski and is currently a doctoral graduate student at Tufts University focusing on NIR spectroscopy. **Kevin Leiva, BS,** is a doctoral student at OIL-FIU. **Richard Schutzman, BS,** was an undergrad research assistant at OIL. **Edwin Robledo, BS,** is an MS student at OIL-FIU. **Penelope Kallis, MD,** worked as a research fellow in the University of Miami (UM) Wound Care Center. **Luis J. Borda, MD,** is a research fellow in the Department of Dermatology and Cutaneous Surgery at the UM Miller School of Medicine (MSM) and Wound Care Center. **Francisco Perez-Clavijo, DPM,** is a podiatric physician and surgeon at Podiatry Care Partners (Miami). **Robert Kirsner, MD, PhD,** is the Chairman (and endowed Harvey Blank Chair) in Dermatology in the Department of Dermatology and Cutaneous Surgery at the UM-MSM; and also serves as director of the UM Hospital Wound Center. **Anuradha Godavarty, PhD,** is an Associate Professor in the Department of Biomedical Engineering at FIU. Her research interests are in developing hand-held and mobile NIR devices for wound care, cancer prognosis, and functional brain mapping.

REFERENCES

1. Maloney C, Lyons G, Burke P, et al. A review of technological approaches to venous ulceration. Rev Biomed Eng 2005;33:511–556.
2. Alavi A, Sibbald RG, Phillips TJ, et al. What's new: management of venous leg ulcers. J Am Acad Dermatol 2016;74:627–640.
3. Rice JB, Desai U, Cummings AKG, et al. Burden of venous leg ulcers in the United States. J Med Econ 2014;17:347–356.
4. Collins L, Seraj S. Diagnosis and treatment of venous ulcers. Am Fam Physician 2010;81:989–996.
5. Simon D, Dix F, McCollum C. Management of venous leg ulcers. BMJ 2004;328:1358–1362.
6. Falanga V, Eaglstein W. The trap hypothesis of venous ulceration. Lancet 1993;341:1006–1008.
7. Etufugh CN, Phillips TJ. Venous ulcers. Clin Dermatol 2007;25:121–130.
8. Gray D, White R, Cooper P, Kingsley A. The wound healing continuum. Br J Community Nurs 2002;7:15–19.
9. Herbin M, Venot A, Devaux JY, Piette C. Colour quantitation through image processing in dermatology. IEEE Trans Med Imaging 1990;9:262–269.
10. Gelfand J, Hoffstad O, Margolis D. Surrogate endpoints for the treatment of venous leg ulcers. J Invest Dermatol 2002;119:1420–1425.
11. Kikta M, Schuler J, Meyer J, Jr., et al. A prospective, randomized trial of Unna's boots versus hydroactive dressing in the treatment of venous stasis ulcers. J Vasc Surg 1988;7:478–483.
12. Fazli M, Bjarnsholt T, Moller K, et al. Nonrandom distribution of *Pseudomonas aeruginosa* and *Staphylococcus aureus* in chronic wounds. J Clin Microbiol 2009;47:4084–4089.
13. Kobrin K, Thompson P, Scheur M, et al. Evaluation of dermal pericapillary fibrin cuffs in venous ulceration using confocal microscopy. Wound Repair Regen 2008;16:503–506.
14. Schuh S, Holmes J, Ulrich M, et al. Imaging blood vessel morphology in skin: dynamic optical coherence tomography as a novel potential diagnostic tool in dermatology. Dermatol Ther 2017;7:187–202.
15. Randeberg L, Denstedt M, Paluchowski L, et al. Combined hyperspectral and 3D characterization of non-healing skin ulcers. In: Proceedings of IEEE Conference on Color and Visual Computing Symposium. Gjovik, Norway: 2013.
16. Denstedt M, Pukstad B, Paluchowski L, et al. Hyperspectral imaging as a diagnostic tool for chronic skin ulcers. Proceedings Volume 8565, Photonic Therapeutics and Diagnostics IX; 85650N (2013) https://doi.org/10.1117/12.2001087.
17. Virgini-Magalhaes C, Porto C, Fernandes F, et al. Use of microcirculatory parameters to evaluate chronic venous insufficiency. J Vasc Surg 2006;43:1037–1044.
18. Basiri A, Nabili M, Mathews S, et al. Use of multispectral camera in the characterization of skin wounds. Opt Express 2010;18:3244–3257.
19. Mlacak B, Blinc A, Gale N, et al. Microcirculation disturbances in patients with venous ulcer

before and after healing as assessed by laser doppler flux-metry. Arch Med Res 2005;36:480–484.

20. Junger M, Klyscz T, Hahn M, et al. Disturbed blood flow regulation in venous leg ulcers. Int J Microcirc Clin Exp 1996;16:259–265.

21. Gschwandtner M, Ambrozy E, Maric S, et al. Microcirculation is similar in ischemic and venous ulcers. Microvasc Res 2001;62:226–235.

22. Stucker M, Huntermann C, Georges F, et al. Capillary blood cell velocity in periulcerous regions of the lower leg measured by laser Doppler anemometry. Skin Res Technol 2004; 10:174–177.

23. Schmidt M, Fassler D, Liebold K, et al. Contact-free spectroscopy of leg ulcers: principle, technique, and calculation of spectroscopic wound scores. J Invest Dermatol 2001;116:531–535.

24. Sayre E, Kelechi T, Neal D. Sudden increase in skin temperature predicts venous ulcers: a case study. J Vasc Nurs 2007;25:46–50.

25. Lei J, Rodriguez S, Jayachandran M, et al. Assessing the healing of venous leg ulcers using a noncontact near-infrared optical imaging approach. Adv Wound Care 2017;7:1–10.

26. Bigio IJ, Fantini S. Quantitative Biomedical Optics: Theory, Methods, and Applications (Chapter 15 Oximetry). Cambridge, England: Cambridge University Press, 2016.

27. Yudovsky D, Nouvong A, Pilon L. Hyperspectral imaging in diabetic foot wound care. J Diabetes Sci Technol 2010;4:1099–1113.

28. Papazoglou E, Neidrauer M, Zubkov L, Weingarten M, Pourrezaei K. Noninvasive assessment of diabetic foot ulcers with diffuse photon density wave methodology: pilot human study. J Biomed Opt 2009;14:064032.

Abbreviations and Acronyms

2D = two dimensional
CURE = Coulter Undergraduate Research Excellence
CW = continuous wave
DFU = diabetic foot ulcer
GUI = graphical user interface
HbO = oxygenated hemoglobin
HbR = deoxygenated hemoglobin
HbT = total hemoglobin
HSI = hyperspectral imaging
LED = light-emitting diode
MBLL = modified Beer-Lambert's law
MSI = multispectral imaging
NIR = near-infrared
NIROS = near-infrared optical scanner
OD = optical density
ROI = region of interest
StO_2 = oxygen saturation
VLU = venous leg ulcer

(*Appendix follows* →)

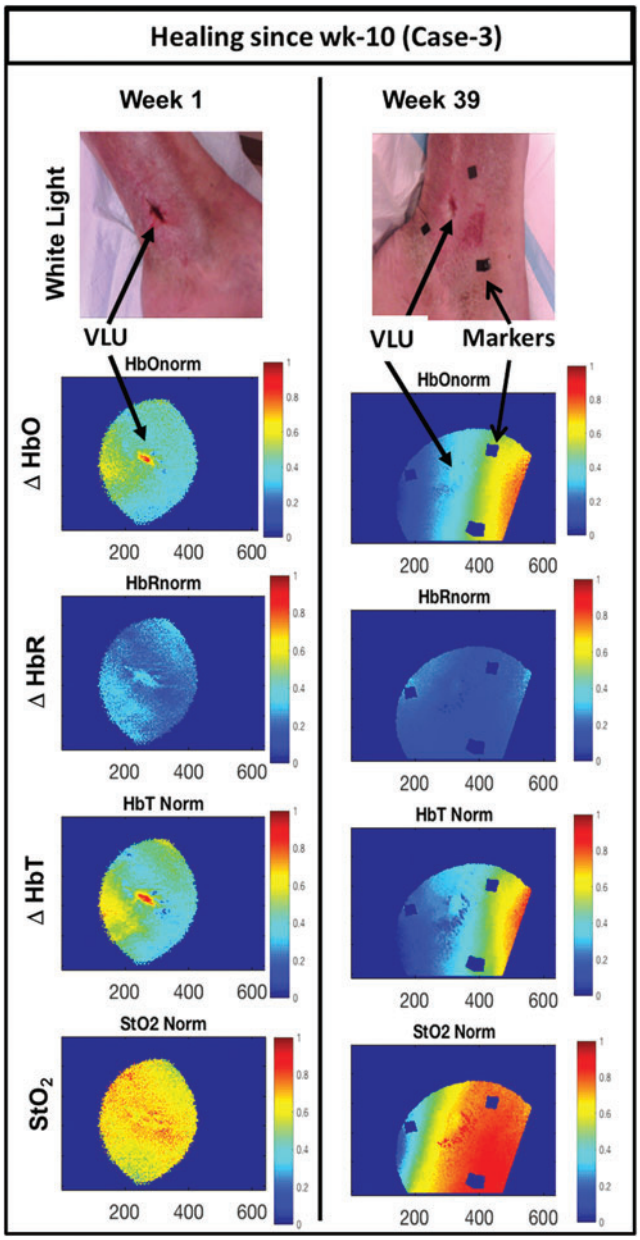

Appendix Figure A1. White light images (*top row*), normalized ΔHbO maps (*second row*), normalized ΔHbR maps (*third row*), normalized ΔHbT maps (*fourth row*), and normalized StO_2 maps (*fifth row*) for healing VLU (case 3) at the first and last week of imaging. Color images are available online.

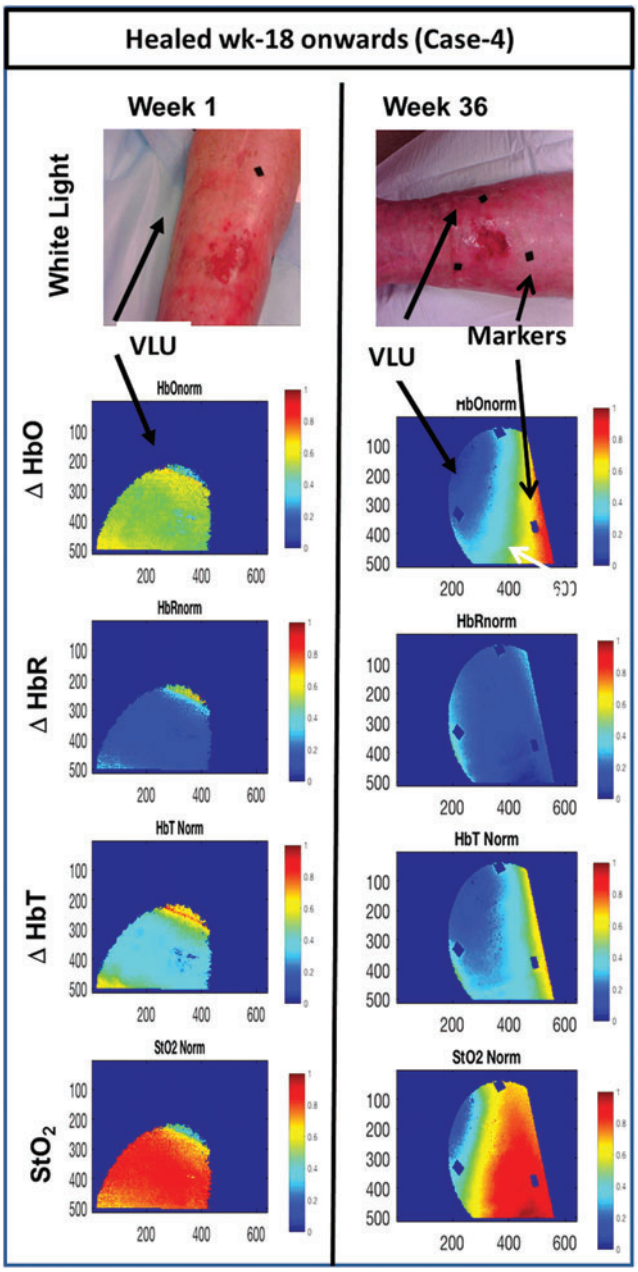

Appendix Figure A2. White light images (*top row*), normalized ΔHbO maps (*second row*), normalized ΔHbR maps (*third row*), normalized ΔHbT maps (*fourth row*), and normalized StO_2 maps (*fifth row*) for healing VLU (case 4) at the first and last week of imaging. Color images are available online.